*J. Anat.* (2002) **200**, pp415–430

REVIEW

# Axons and glial interfaces: ultrastructural studies*

John Fraher

*Anatomy Department, Biosciences Institute, University College Cork, Cork, Ireland*

## Abstract

At most vertebrate nerve transitional zones (TZs) there is a glial barrier which is pierced by axons passing between the CNS and PNS. Myelinated axons traverse this in individual tunnels. The same is true of larger non-myelinated axons. This holds widely among the vertebrates, for example, the large motor axons of the sea-lamprey *Petromyzon* (which also possess TZ specializations not found in mammals). Smaller non-myelinated axons traverse the TZ glial tunnels as fascicles and so the barriers are correspondingly less comprehensive for them. Accordingly, in nerves composed of non-myelinated axons, such as the vomeronasal or the olfactory, a TZ barrier stretching across the nerve is effectively absent. The chordate *Amphioxus* differs from the vertebrates in lacking a TZ barrier throughout. Invertebrates also lack glial barriers at the TZs between ganglia and interconnecting nerve trunks. The glial barrier at the dorsal spinal root TZ (DRTZ) has considerable value for analysing protocols aimed at achieving CNS regeneration, because it provides a useful model of the gliotic reaction at sites of CNS injury. Also, it is especially amenable to morphometric analysis, and so enables objective quantification of different protocols. Being adjacent to the subarachnoid space, it is accessible for experimental intervention. The DRTZ was used to investigate the value of neurotrophin 3 (NT3) in promoting axon regeneration across the TZ barrier and into the CNS following dorsal root crush. It promoted extensive regeneration and vigorous non-myelinated axonal ensheathment. On average, around 40% of regenerating axons grew across the interface, compared with virtually none in its absence. These may have traversed the interface through loci occupied by axons prior to degeneration. Many regenerating axons became myelinated, both centrally and peripherally.

**Key words** CNS–PNS transitional zone; comparative; regeneration.

## Axon–glial relationships at the CNS–PNS transitional zone

Every nerve that is attached to the neuraxis has a transitional zone (TZ) (Fig. 1). In the vertebrates, most TZs examined have a glial partition stretching across the nerve bundle. This forms the PNS–CNS boundary and is pierced by the axons as they cross between the CNS and PNS (Fraher, 1992). There is a sharp discontinuity of tissue types at the TZ. The myelinating glia meet at the transitional node, the features of which are a composite of those of central and peripheral nodes (Fraher & Kaar, 1984). The principal supporting tissues are astrocytes centrally and endoneurium peripherally. The interface between the two *milieux* lies at the surface of the CNS and consists of the superficial plasmalemmae of the mosaic of astrocyte processes which form the surface of the glia limitans (Berthold et al. 1984; Fraher & Rossiter, 1990). This is covered by a basal lamina, which in turn is continuous with each of the sleeves forming the inner elements of the endoneurial tubes around the nerve fibres in the PNS. At the TZ the CNS tissue extends distally into most roots as a tapering central tissue projection. The astrocytic covering of the TZ is a thickening of the glia limitans generally.

Axons penetrating the glial barrier comprised by the TZ glia limitans come to do so at a very early stage of

Correspondence
*Professor J. Fraher, Anatomy Department, Biosciences Institute, University College, Cork, Ireland. Tel. +353 21 4902115; fax: +353 21 4273518; e-mail: j.fraher@ucc.ie*

**From a paper presented at a one-day symposium on Peripheral Nerve and Neuropathies, to celebrate the contribution of P.K. Thomas as Editor of the Journal of Anatomy 1990–2001, at the Institute of Neurology, Queen Square, London, UK, 22 March 2002.*

Accepted for publication *1 March 2002*

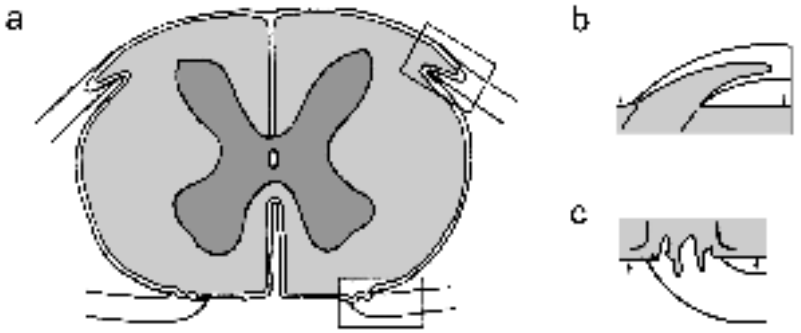


**Fig. 1** Diagrams with enlargements of the areas outlined, showing (a) transversely sectioned spinal cord, (b) dorsal root attachment to the spinal cord, in which the rootlet contains a central tissue projection, (c) ventral root attachment to the spinal cord. Both show interdigitation of CNS and PNS tissues along the length of rootlet termed the transitional zone (TZ). Pale: PNS tissue; intermediate: CNS white matter; dark: CNS grey matter; Spinal cord surface: arrows.

its development, as at the developing ventral roots (O'Brien et al. 1998, 2001). Here, outgrowing motoneurone axons emerge through the mosaic of processes forming the thin, primitive glia limitans (Fig. 2a). The axons of the bundles themselves are naked and are apposed to one another at first. They are secondarily segregated by fine astrocytic processes which grow in from outside the margins of the bundle (Fig. 2b,c). These become progressively more elaborate and form the thick, highly complex mosaic which characterizes the TZ glia limitans. As a result of the segregation process, myelinated axons cross the TZ barrier singly. The point at which they pierce the glia limitans coincides with the locus of the transitional node. Most non-myelinated axons cross the TZ in a different way. They do so as bundles, in which the individual axons are not segregated from each other. Consequently, the glial barrier is less well developed in relation to these, compared with the crossing points of those which are myelinated. In those nerves which are composed of large bundles of non-myelinated axons, such as the vomeronasal (Fraher, 1982) (Fig. 3) or the olfactory, the TZ barrier is effectively absent. Here the arrangement at maturity resembles that of an early, developing nerve. Indeed, during vomeronasal nerve development, bundle size, in terms of the number of axons per bundle, actually increases. This developmental trend is thus the opposite of that which takes place in typical peripheral nerves, which are characterized by progressive segregation towards a one-to-one ratio between Schwann cells and the ensheathed axon segments. In these special cases therefore the interstitial, interaxonal spaces continue uninterrupted between CNS and PNS. The structural seal is therefore less tight than for the transitions of myelinated axons. The layer of ensheathing glia of the vomeronasal nerve is continuous with the glia limitans of the accessory olfactory bulb (Fraher, unpublished observations). This arrangement is likely to be similar to that described for the olfactory nerve glia (olfactory ensheathing cells – OECs) (Doucette, 1984, 1991, 1993). A TZ glial barrier is thus effectively absent in these two nerves in those mammals investigated so far.

The Schwann cells of typical myelinated fibres have only very limited contact with glia limitans astrocytes at the TZ. This contact, where it takes place at all, does so at the transitional node gap, and consists of apposition of Schwann cell microvilli to astrocyte processes projecting into the gap (Fraher & Kaar, 1984). In this location the two tend to be separated by basal lamina (Fig. 4a). By contrast, Schwann cell – astrocyte contact is more in evidence at the transitions of non-myelinated axon bundles (Fig. 4b). Here, the Schwann cell sheath is directly apposed to astrocyte processes over a short distance central to the level at which the basal lamina is reflected between the two (Fraher & Rossiter, 1990). Some of the larger non-myelinated axons traverse the glial barrier individually, rather like those which are myelinated. Myelination therefore seems to be associated with the least degree of apposition and possibly therefore with the greatest degree of repulsion between the two cell types.

Extensive Schwann cell – glial contact would seem to be the case widely for non-myelinated axon transitions, as exemplified by the mode of transition in the Cyclostome, *Petromyzon* (Fraher & Cheong, 1995). Here, the TZ possesses a clearly defined glial barrier at the plane of the CNS surface (Fig. 5a). This is continuous with the surrounding glia limitans. It is somewhat thicker than the glia limitans generally, a feature in which it resembles the mammals. Also as in the mammals, it stretches across the nerve bundle. Most lamprey axons are unmyelinated and of relatively large calibre. They traverse the TZ in individual glia-lined tunnels. In this they resemble the large non-myelinated and myelinated mammalian axons. *Petromyzon* thus follows the general vertebrate pattern in this regard. In sharp contrast

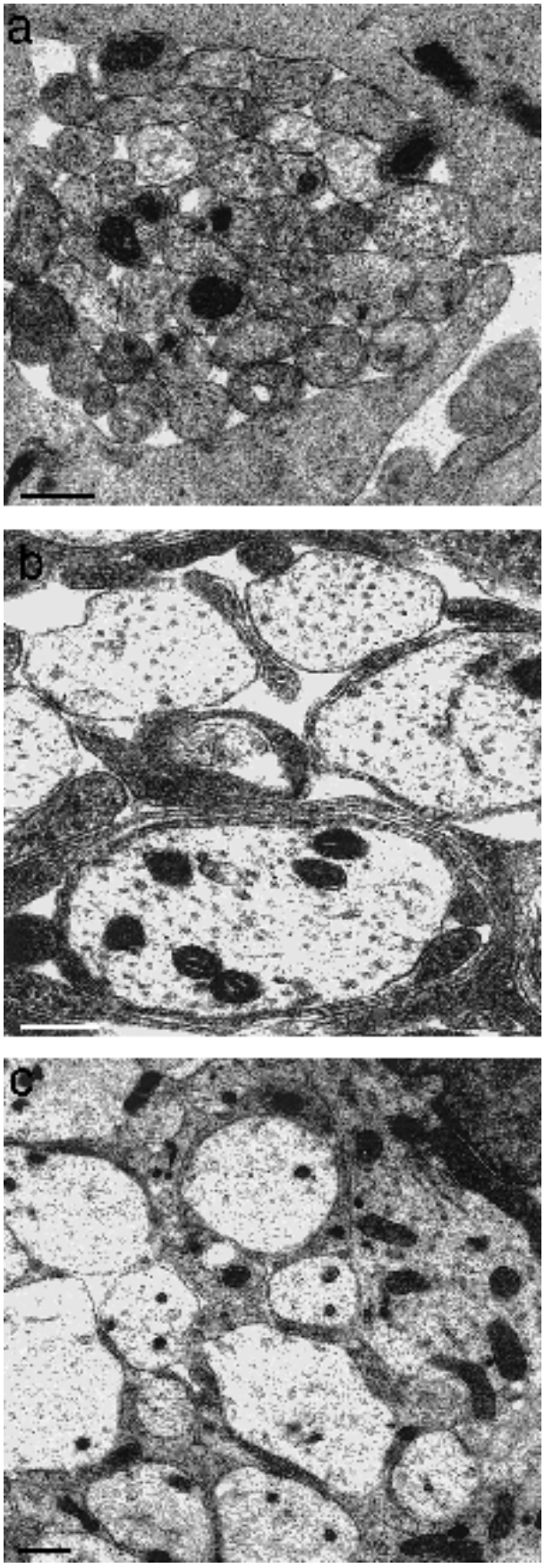


to non-myelinated fibre transitions in the mammals, however, the lamprey TZ demonstrates significant complexity of its Schwann cell – glial relationships. The transitional Schwann cell, which enfolds the axon immediately distal to its emergence from the cord, commonly lies in a depression of the cord surface (Fig. 5d). However, the most striking feature is the presence of an extensive periaxonal labyrinth of spaces around the axon immediately superficial to where it emerges from the cord (Fig. 5c). This is bounded by the axon, the TZ glial processes, multiple Schwann cell processes and the associated basal laminae. Fine Schwann cell processes project into it. This remarkable complex possesses some features resembling those of the mammalian node gap, for example, the interstitial spaces bounded by the basal lamina externally and the axolemma internally, and which are exposed to extensive areas of plasmalemma. The complexities of the lamprey TZ would seem not to be stages in the evolution towards mammalian nodes. Instead, they are specializations which are peculiar to the lamprey, as far as is known at this stage. The glial processes of the lamprey TZ themselves possess specializations not typical of mammals. These include multiple interconnected strata of microfilament bundles which are linked to the surface plasmalemma by hemidesmosomes and which extend deeply into the spinal cord along radially orientated glial processes (Fig. 5b).

Although the range of species studied is limited, it seems likely that all vertebrates possess glial barriers at their typical CNS–PNS TZs. Exceptions are found in certain cases such as the vomeronasal and olfactory nerves. To investigate the wider occurrence or otherwise of a TZ glial barrier, Amphioxus (*Branchiostoma lanceolatum*, Cephalochordata) was studied (Fraher, unpublished observations). The only nerves which are continuous with the spinal cord of Amphioxus are attached to its dorsolateral aspect and correspond roughly in position to mammalian dorsal roots, though they contain both afferent and efferent fibres (Fig. 6a). Motoneurone axons do not leave the cord to form roots. Instead they run rostrally and caudally as bundles

**Fig. 2** At the developing TZ, presumptive large axons are (a) at first naked and emerge between loosely packed processes of the primitive glia limitans (above and below). (b,c) They become progressively segregated from one another by astrocytic processes which grow in from the surrounding cord surface (from Fraher, 1997). Scale bars: a: 1.0 μm; b,c: 0.5 μm.

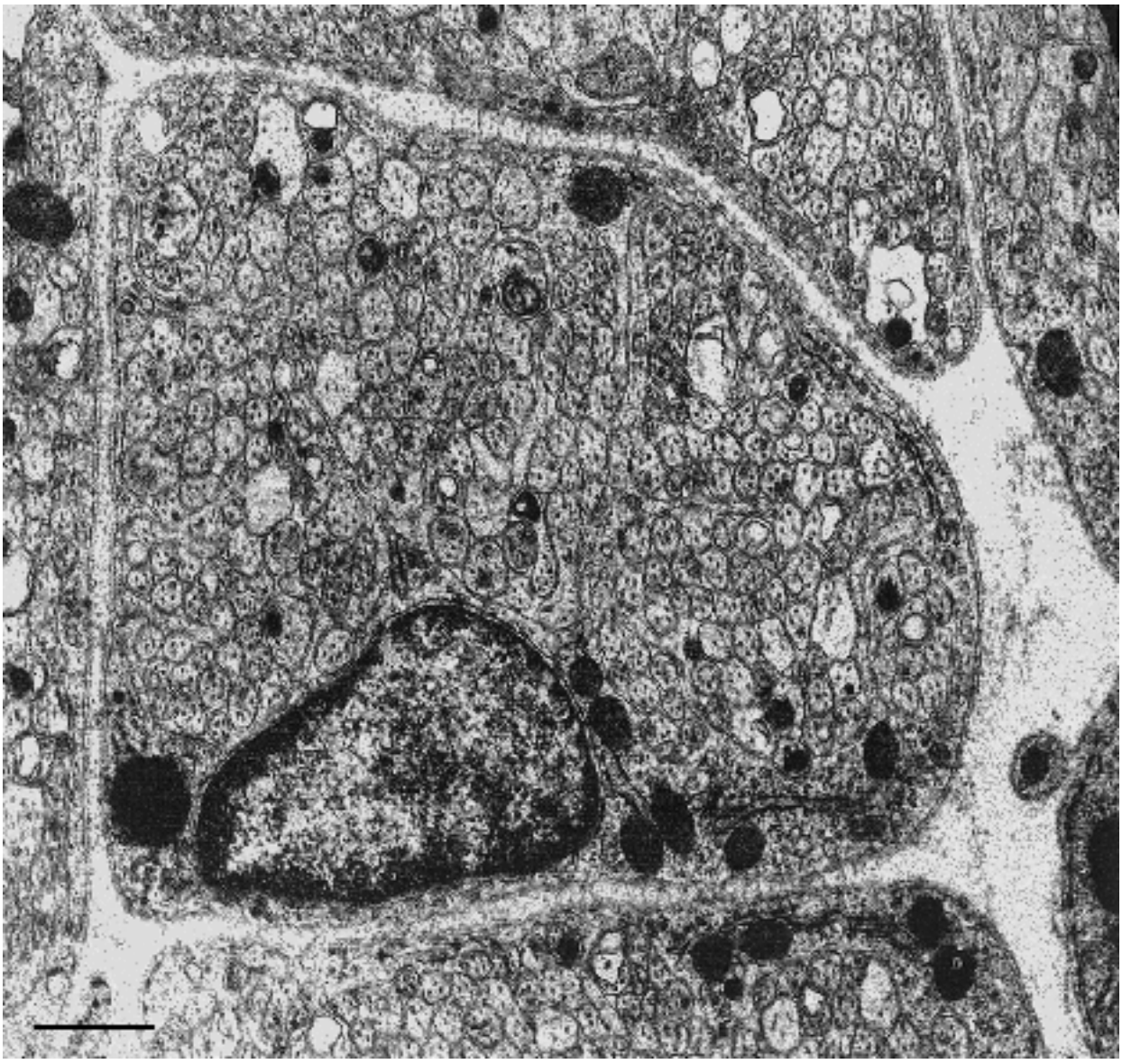

**Fig. 3** Transversely sectioned vomeronasal nerve fascicle, showing it to be composed of large numbers of closely packed small axons, enveloped by a composite sleeve of ensheathing cells which segregate the axon bundle only to a limited extent. Scale bar: 0.5 μm.

which lie immediately deep to the ventrolateral cord surface (Fig. 6b) (Flood, 1966, 1968; Fritsch & Northcutt 1993). Here, synapses resembling complex, wide neuromuscular junctions are formed, through deficiencies in the glia limitans, with processes of the myotomal muscle fibres. Further, similar contacts are made more ventrally with specialized muscular elements associated with the notochord through deficiencies in the notochordal sheath (Fig. 6b). At these, terminals of propriospinal axons within the cord are separated only by a synaptic cleft about 0.5 μm deep from the postsynaptic membrane of the muscular elements (Fig. 6c,d). *Amphioxus* differs from all vertebrates studied to date in lacking any clearly defined glial barrier marking a CNS–PNS transition. Each of its dorsal nerves, however, possesses a transitional segment near its attachment to the cord. Here, glial profiles (perikarya and processes) found among the neurites are increased in frequency relative to more distal levels of the root (Fig. 6a). Though many of the processes are orientated transversely to the long axis of the root, they do not form a continuous central–peripheral barrier. Their frequency declines in a distal direction over the transitional segment to levels typical of the PNS generally.

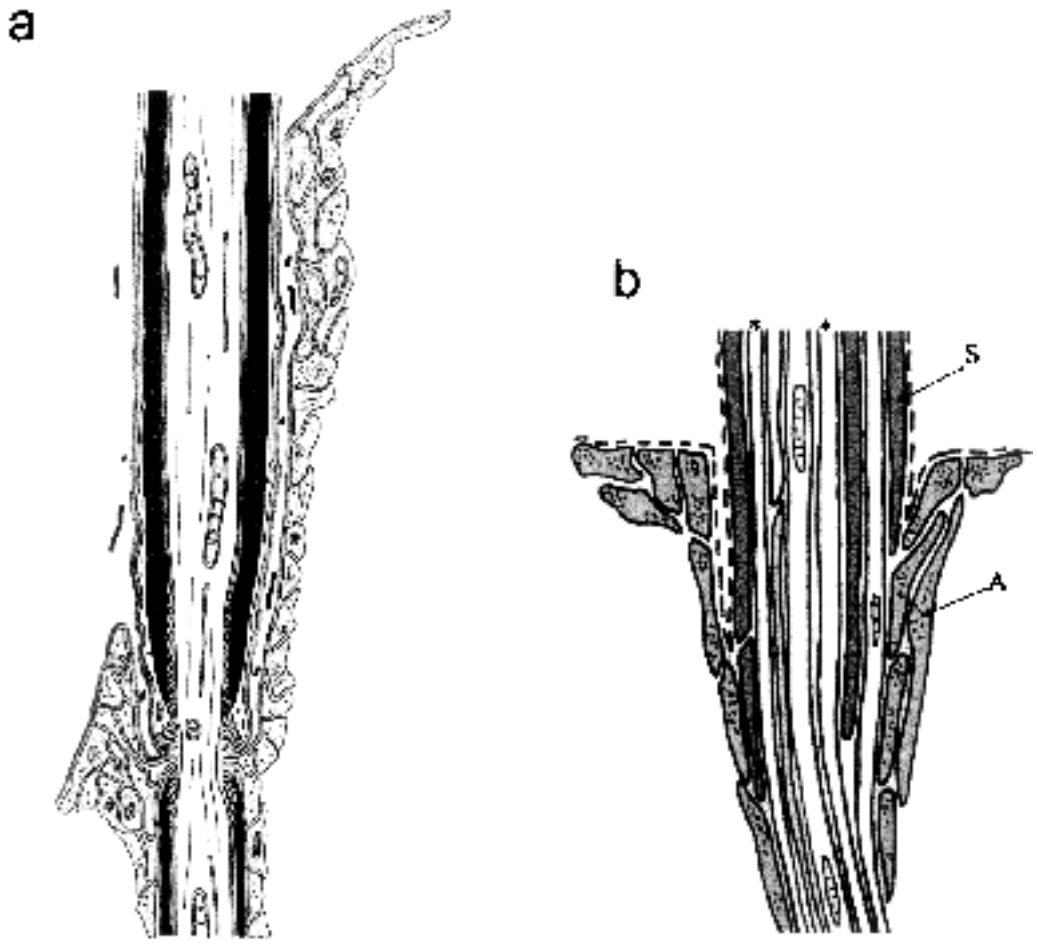


**Fig. 4** Diagram showing the relationships between Schwann cells, astrocytes and axons at the TZ (a) in relation to a myelinated axon at the mature TZ and (b) in relation to a bundle of non-myelinated axons passing through the CNS–PNS interface (see text). (a) Astrocyte processes grey. (b) S: Schwann cell processes; A: astrocyte processes; dashed lines: basal lamina; asterisks: axons.

Invertebrate nervous systems vary considerably. However, many include ganglia with interconnecting nerve trunks. The possibility of there being a glial barrier where these join was investigated (Fraher, unpublished observations). The range of species studied was of necessity not comprehensive. However, it included earthworms and woodlice, as well as several insect and mollusc species. The junctions between the various types of ganglia and the connecting nerve cords were generally clearly evident. The layers of ensheathing cells of both were in continuity and the transitional zones were well defined. However, no clearly defined barrier between the two was found in any case (Fig. 7a–c).

## Regeneration through the transitional zone

Glial barriers have another side to them, as it were. This concerns axon regeneration in the CNS. Part of the reason why axons fail to regenerate in the mammalian CNS following interruption is the formation of an astrocytic scar at the lesion site. The TZ can provide considerable insight into the success or failure of axon regeneration in relation to these reactive astrocytes. In this context, the dorsal spinal nerve root TZ (DRTZ), as well as being of interest as a biological interface with a distinctive and variable geometry, has proven to hold considerable potential for analysing this problem, which is of major significance for clinical neuroscience. Central axons fail to regenerate following interruption, despite attempts to do so (Carlstedt, 1985a, 1985b, 1997; Carlstedt et al. 1988). As in the PNS, central axons attempt to re-grow following interruption, but the regenerative sprouts are largely unsuccessful. Success is more readily achieved in immature animals (Carlstedt, 1988; Carlstedt et al. 1987), or using embryonic material transplanted into the mature nervous system (Kozlova

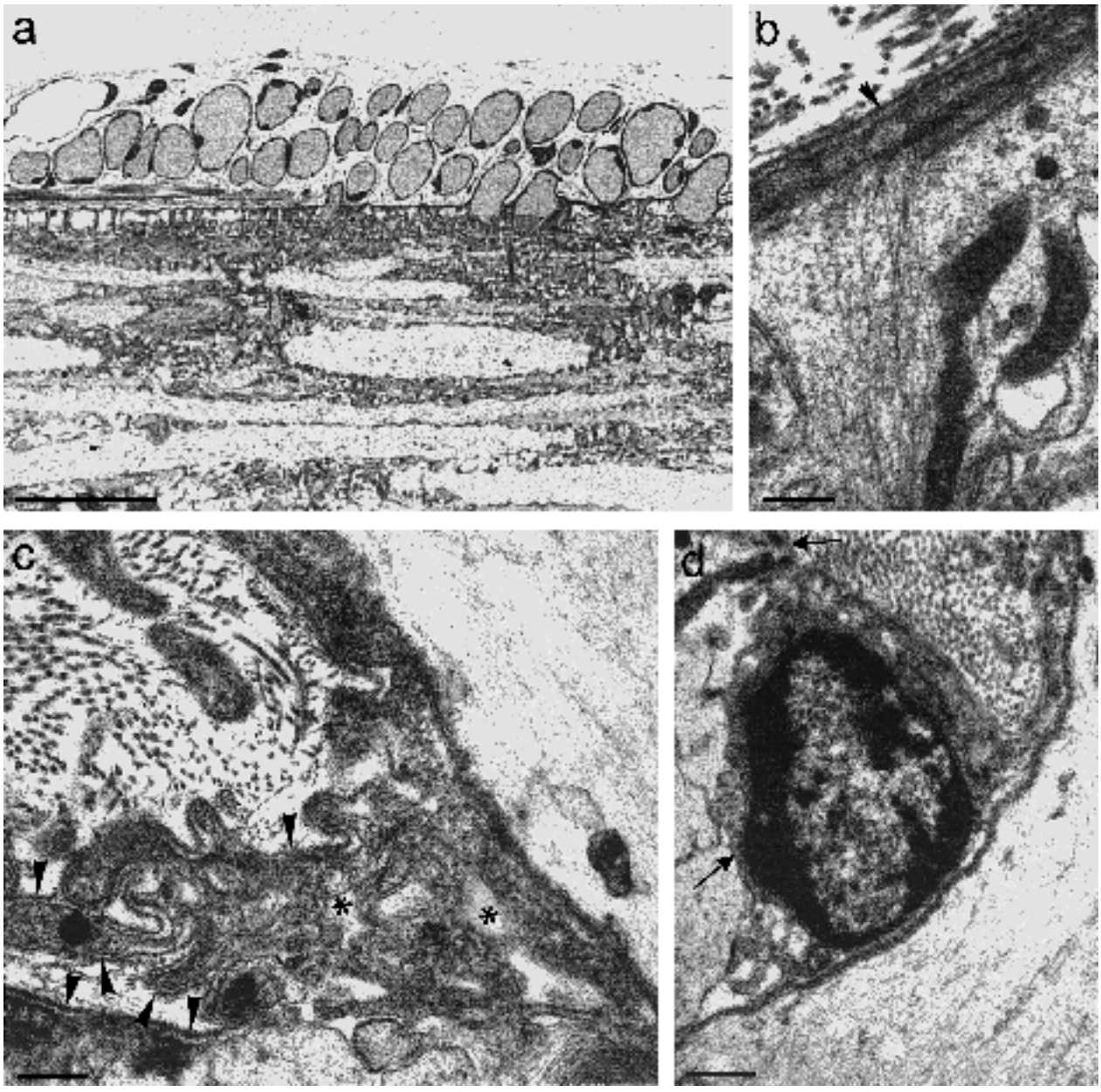


**Fig. 5** (a) Light micrograph of a longitudinal section of a lamprey spinal cord, showing transversely sectioned axons adjacent to, and traversing, the cord surface. Outside the cord each is surrounded by a thin, dark rim of Schwann cell cytoplasm. Scale bar: 50 μm. (b) Electron micrograph showing a dense layer of filaments in a surface process of the glia limitans (above), which extend deeply into its radially orientated extension. (Arrowhead: basal lamina) (from Fraher & Cheong, 1995). Scale bar: 0.25 μm. (c) Electron micrograph showing Schwann cell processes, astrocytic processes and basal lamina (arrowheads) bounding a complex labyrinth of spaces (asterisks) in relation to the axon (above, right) and the glia limitans (below). Schwann cell and astrocyte processes are not separated by basal lamina in the vicinity of the axon (below, right). (From Fraher & Cheong, 1995). Scale bar: 0.5 μm. The perikaryon of a Schwann cell lies in a depression in the glia limitans surface (arrows). The associated axon lies to the right. Scale bar: 0.5 μm.

et al. 1995, 1997). The lack of a structure equivalent to the endoneurial tube in the CNS plays a major part in this because of the resulting lack of a guidance pathway for the regenerating axons. Several other factors contribute to this failure, however. These include oligodendrocytic myelin breakdown products (Caroni & Schwab, 1988a, 1988b; Schnell & Schwab, 1990; Pindzola et al. 1993; Schwab, 1996a, 1996b; Guest et al. 1997; Schwab & Brosamle, 1997; Spillmann et al. 1997; Tatagiba et al. 1997), which may inhibit an inherent

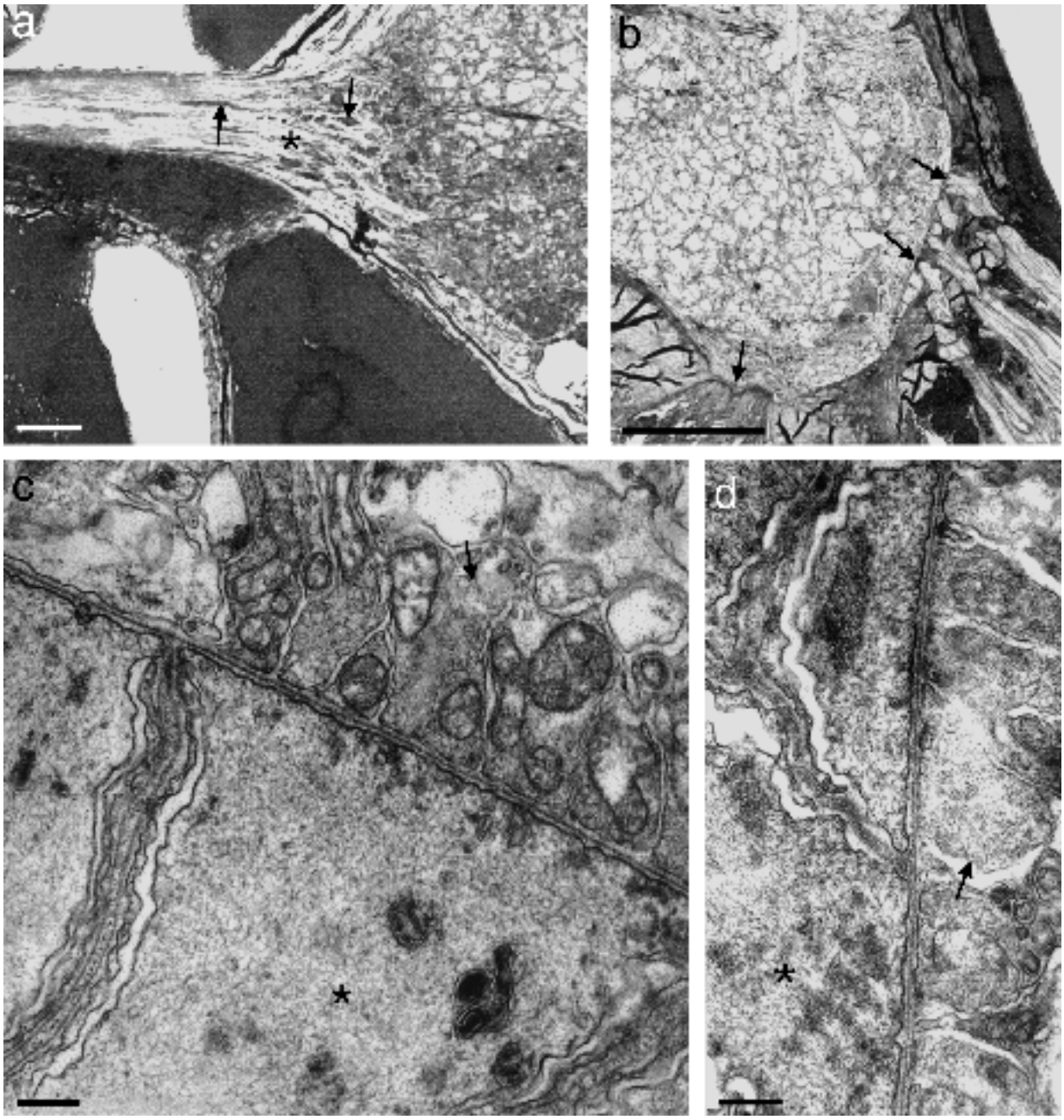


**Fig. 6** (a,b) Transverse sections of the spinal cord of *Amphioxus*. (a) The dorsal nerve extends to the left from the dorsolateral aspect of the cord. At its attachment there is no glial barrier. However, glial perikarya (arrows) are most densely packed in the region of the tapering transitional segment (asterisk). Their density decreases progressively in a central–peripheral direction. (b) In the ventrolateral part of the cord, its surface is closely related to muscle elements (arrows): laterally to processes of myotomal muscles and more medially to notochordal muscle-like processes. The glia limitans is deficient at both locations and the notochordal sheath is deficient at the second. Scale bars: 25 μm. (c,d) Electron micrographs of the apposed cord surface and muscle elements in the above locations, showing contacts resembling complex, wide neuromuscular junctions between the two. Here, terminals of propriospinal axons within the cord (arrows) are separated by a synaptic cleft about 0.5 μm deep from the muscle-like fibres (asterisks). Scale bars: 0.5 μm.

tendency for sprouting of non-lesioned neurites (Thallmair et al. 1998). Another factor of major importance is the gliotic reaction (see Fraher, 2000 for review). Astrocyte processes at the injury site play a major role in this by contributing to the scar at the lesion site. The response of the TZ to dorsal root injury forms a useful model of these events. During the degeneration–regeneration sequence, the TZ glial barrier does not

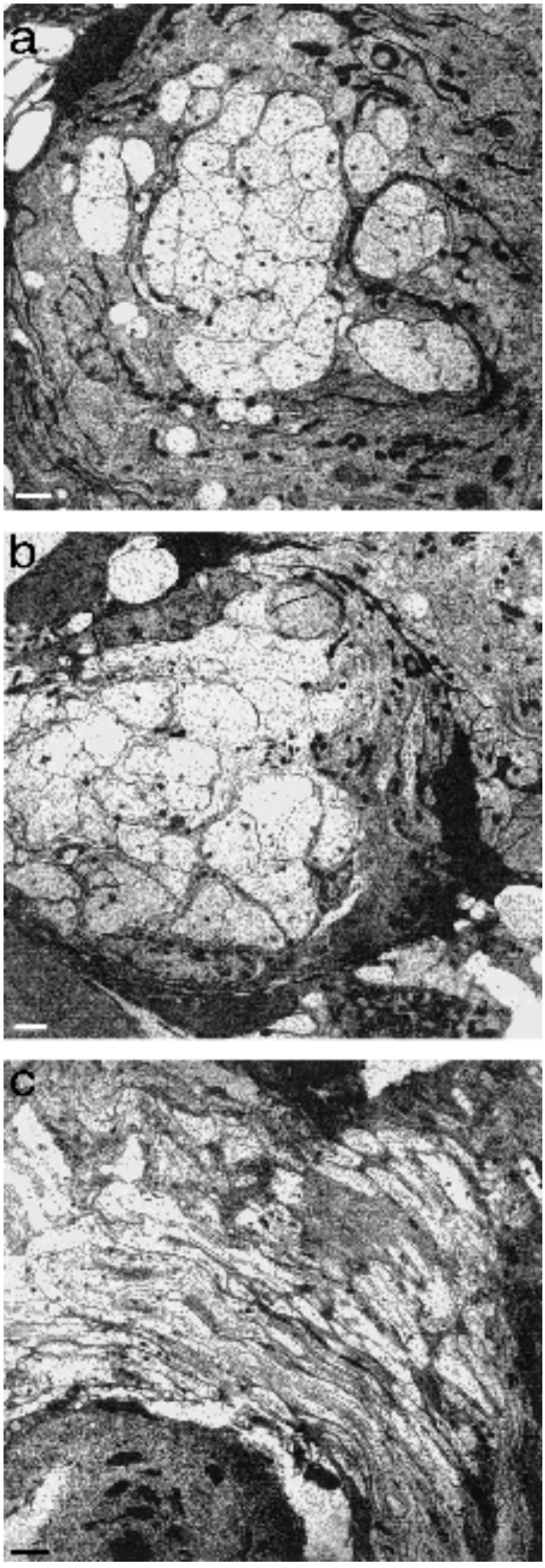


break down. Nor do the tunnels formerly occupied by degenerated axons permit axon regeneration in a central direction through them. On the contrary, the TZ astrocyte processes proliferate and contribute to a glial scar which, untreated, inhibits regeneration and prevents the regenerating axons from growing into the CNS, by both physical and molecular means (Carlstedt et al. 1989; Bovolenta et al. 1992, 1993). The astrocytic outgrowth extends distally into the dorsal root for a considerable distance (Liu & Kozlova, 2000).

In using the DRTZ as a model in which to study axon regeneration, the objective is to induce axons to grow from the PNS into the CNS through TZ astrocytic tissue which is undergoing gliosis following dorsal root fibre interruption central to the ganglion. The DRTZ has several advantages in this regard. Firstly, attempts at regeneration can be compared peripheral to, central to and within the reactive glial tissue. In the first of these locations conditions are relatively favourable towards it, in the other two they are less so. Secondly, the environment of the TZ is adjacent to the subarachnoid space, and so is relatively accessible for experimental intervention. As a result, conditions in the environment of the lesion can be altered in ways designed to enhance or otherwise modify regeneration. Thirdly, such environmental change can be brought about without unwanted damage to central tissue, which is much more difficult to achieve when lesioning the CNS, because gaining access there necessarily results in accessory damage to tissue at sites other than that of the lesion. Fourthly, the DRTZ has the major advantage of being especially amenable to morphometry. Both the PNS and CNS tissues of the TZ and of the adjacent regions of the nerve roots and the dorsolateral spinal cord are ideal for quantitative analyses such as axon counting, myelin sheath thickness measurements, and morphometry of glial and glial scar tissue during both degeneration and regeneration. In studies on regeneration, corresponding parameters in both locations can be readily measured and compared. This enables various indices of regeneration to be calculated, such as percentages of regenerating axons crossing the TZ interface, or comparative

**Fig. 7** Electron micrographs of cockroach nervous tissue. (a,b) Semiserial transverse sections through the same axon bundle (a) peripheral to a nerve ganglion and (b) where it enters the ganglion. There is no evident glial barrier crossing the axon bundle. (c) Longitudinal section through an axon bundle entering a nerve ganglion, from below, right to above, left. No glial barrier crosses the axon bundle. Scale bar: 5 μm.

measurements of axon calibre or myelin sheath thickness in the two locations. An additional advantage of the DRTZ model is that, unlike central fibre tracts, the rootlet has clearly defined boundaries (Fig. 1). As a result, there need be no uncertainty about the limits of the experimental tissue.

Using the DRTZ protocol, axon regeneration along the dorsal root and into the TZ was investigated under two sets of conditions: in the absence of any neurotrophin, and in the presence of Neurotrophin 3 (NT3). NT3 was delivered intrathecally to the lesion site following root crush in adult rats under appropriate anaesthesia. Specimens were prepared by Ramer and his co-workers following their defined experimental protocols (Ramer et al. 2000). Recovery was followed by axonal regeneration centrally through the dorsal root and its constituent rootlets and into the CNS. Regeneration was assessed 1 week after the lesion as the growing axons interacted with the glial tissues of the TZ. Responses were compared with those taking place in the absence of neurotrophin. The studies focused on the ultrastructural features of degeneration and regeneration in the DRTZ, from morphological and morphometric perspectives. Other linked studies involved immunohistochemical, immunoelectron microscopical and physiological analyses of equivalent material from the same series of experimental animals (Ramer et al. 2000, 2002).

Typical features of degeneration were evident in both CNS and PNS compartments. These included axon degeneration and phagocytosis, as well as those of myelin breakdown such as lamellar separation and disruption, sheath fragmentation and the appearance of lipid inclusions. Degenerative features were more prominent in the CNS than in the PNS at any given stage, indicating that the process, including removal of myelin breakdown products, takes place much more slowly in the former than in the latter.

The PNS compartment possessed large numbers of regenerating axons, mostly non-myelinated, in both protocols (Fig. 8a). A minority showed evidence of the onset of myelination or possessed thin myelin sheaths (see below). In the presence of NT3, non-myelinated axonal ensheathment was more vigorous than in its absence. The fibres demonstrated a wide variety of mesaxonal appearances, typical of early peripheral myelination in developing rat spinal nerve roots (Friede & Samorajski, 1968; Williams & Wendell-Smith, 1971; Fraher, 1973). NT3 is associated with enhanced axonal ensheathment by Schwann cells in the regenerating PNS environment.

Glial fringe complexes extended distally from the CTP among the regenerating fibres (Fig. 8b). In these, Schwann cell profiles and astrocytic processes were extensively apposed to one another within common basal lamina tubes. The Schwann cell elements included both perikarya and processes. This direct Schwann cell – astrocyte apposition is much more extensive than that normally found in the mature TZ. This marked increase in contact does not necessarily entail any topological change in the essential relationship of the two cell types at the TZ. It probably comes about as a result of distal extension of the astrocyte processes through the locus of the erstwhile node gap and within the sleeve of basal lamina to occupy the space vacated by the degenerating axon and the retracting Schwann cell as the latter loses its myelin sheath (Fig. 9). The marked increase in the extent of Schwann cell – astrocyte apposition suggests that any mutual repulsion between them is lessened, compared with the normal state.

In the absence of neurotrophin only very occasional axons, some of which were myelinated, were seen in the CNS compartment. A high proportion of these were small myelinated axons which had relatively thick sheaths. Fibres with similar dimensions were not seen in the PNS. These may have been propriospinal axons which were taking an aberrant, looping course through the TZ, and which did not cross the TZ glial boundary. Fibres with such courses are occasionally seen in normal TZs (Fraher & Bristol, unpublished observations). In marked contrast, in the presence of NT3, axons were commonly found within the CNS compartment of the TZ (Fig. 8c,d). These regenerating axons tended to be separated by astrocyte processes from persistent myelin debris. At CNS levels most regenerating axons were non-myelinated and were associated with astrocyte processes only. However, in some instances oligodendrocytic profiles were apposed to the axons (Fig. 8c) and some of these showed features of incipient or early myelination (Fig. 8d). In the presence of NT3, regenerating axons crossed the CNS–PNS barrier in a distinctive way (Fig. 10a). Many were enfolded by a very short, rounded Schwann cell perikaryon. This, and its ensheathing processes, which extended deep to the plane of the CNS surface, were closely apposed to the glia limitans without intervening basal lamina (Fig. 10b,c). Its appearance was reminiscent of the lamprey Schwann cells found in a similar relationship to the cord surface, and which formed

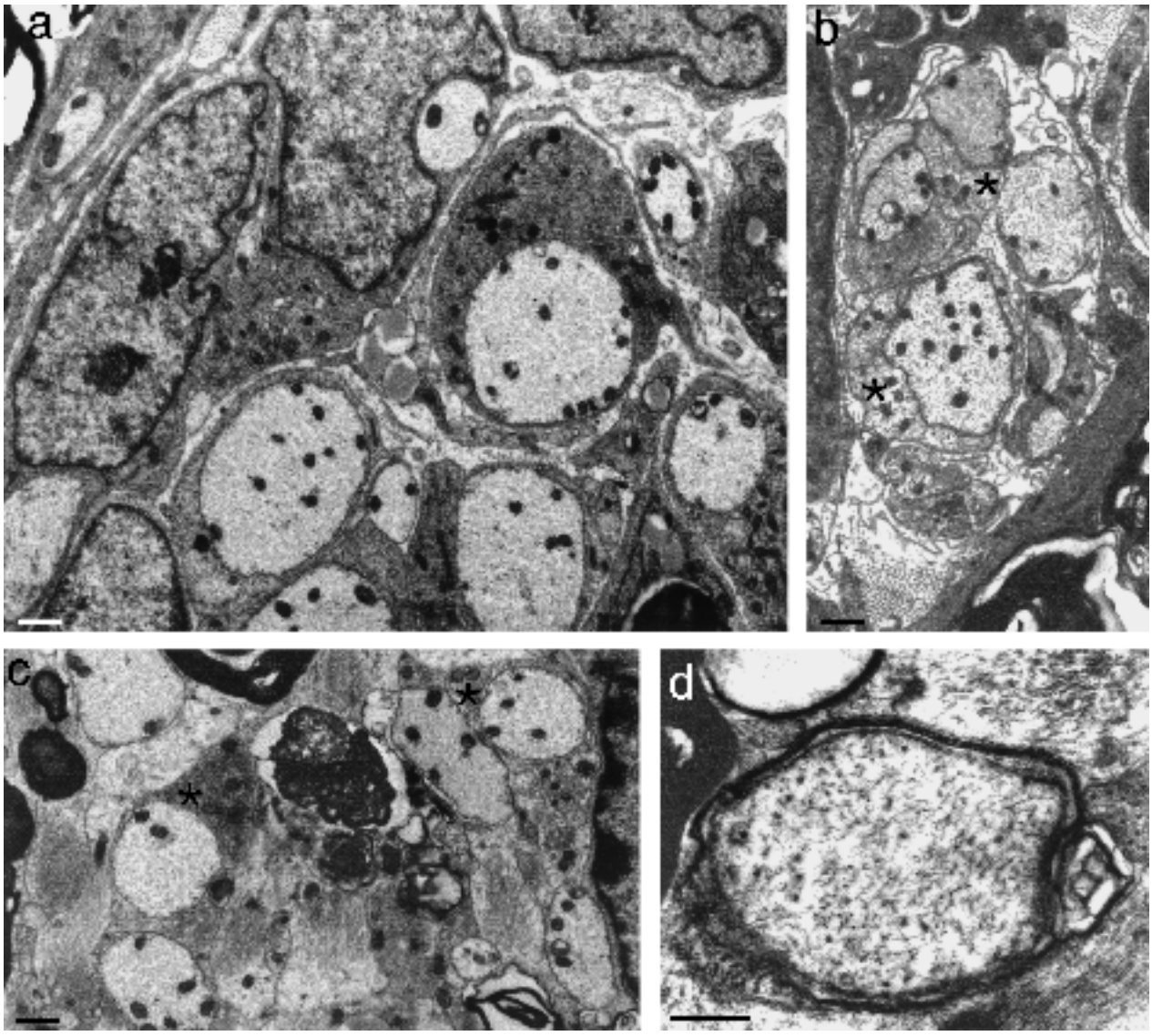


**Fig. 8** (a) Electron micrograph of a transversely sectioned NT3-treated dorsal rootlet at PNS level, showing ensheathment of regenerating axons by Schwann cells. (b) Electron micrograph of a transversely sectioned dorsal rootlet showing a glial fringe complex extending distally into PNS territory and consisting mostly of astrocyte processes (asterisks) enfolding regenerating axons. (c,d) Electron micrographs of transverse sections of rootlets at central levels showing axonal profiles, including (c) some with apposed oligodendrocyte processes (asterisks); others (d) had thin compact myelin sheaths. (b: from Fraher & Dockery, 2002). Scale bars: 0.5 μm.

the complexes referred to above (Fig. 5d). The vigorous regenerative behaviour at PNS levels is therefore consistent with effective axonal invasion of the CNS and the establishment of functional contacts there, which was found in parallel functional studies (Ramer et al. 2000).

The extent of axon regeneration in this study was assessed in two ways: by nerve fibre morphometry in the PNS and CNS tissue compartments of the rootlets, and from axon counts at levels immediately distal and central to the CTP. The degree and rate of regeneration was also assessed in terms of axon calibre and myelin sheath thickness. Myelin–axon regression relationships were used in order to estimate the degree of remyelination, compared with control mature adult values. By 1 week after crush, many of the regenerating NT3-treated axons had begun to acquire myelin sheaths, both centrally and peripherally. These were still relatively thin, most being composed of 10 lamellae or fewer (Fig. 8d). The early stage of their myelination was evident from the scattergrams relating their sheath thickness to axon calibre (Fig. 11). These had regression lines of virtually zero slope. The marked differences

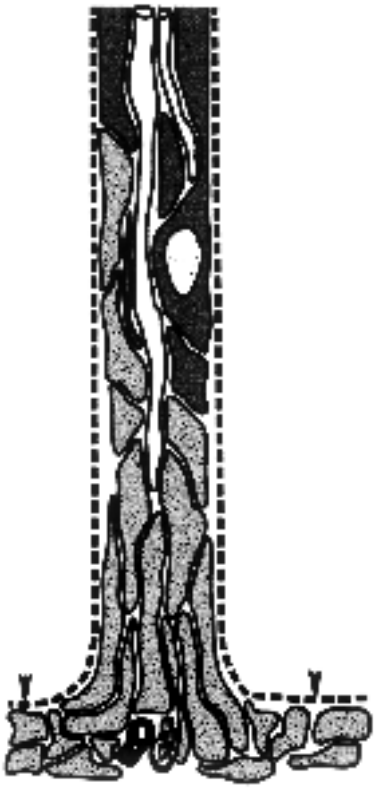

**Fig. 9** Diagram showing a Schwann cell – astrocyte complex (see text) and the relationships between Schwann cells (black), astrocytes (grey) and axons (white). The astrocyte processes of the complex extend distally from the CNS in an endoneurial tube which formerly contained a myelinated axon. (From Fraher & Dockery, 2002). Arrowheads: CNS surface.

between these distributions and those of the undamaged adult controls enabled immediate distinction of the two fibre classes. The correlation between sheath thickness and axon diameter was significant in controls, but not in regenerating fibres in either the PNS or the CNS. For the latter this clearly reflects the very early stage of their myelination (Fraher et al. 1988). Their axon calibre varied considerably, while their myelin sheaths were uniformly very thin. The course of their subsequent growth and maturation remains to be elucidated. For the undamaged controls, the strength of the correlation and also the proportion of sheath thickness variance which can be explained by a linear relationship to axon calibre (the coefficient of determination) (0.6 for PNS and 0.5 for CNS fibre populations) were typical of mature myelinated fibre populations in both locations. In the NT3-treated tissue, regenerating axon diameter had similar distributions in both PNS and CNS compartments (Fig. 12) and almost identical means of approximately 1.3 μm.

The extent of axon regeneration across the CNS–PNS interface was also used to estimate the efficacy of NT3 treatment. To do this, axon numbers were estimated at 1 week following crush, immediately central and peripheral to the TZ. The counts enabled indices of regeneration to be calculated, as the ratios of axon numbers central and peripheral to the CTP in each of several rootlets. The results show that a substantial proportion of axons grow across the interface. Evidence for regeneration was found in all NT3-treated rootlets, though indices for individual rootlets ranged widely (0.04–0.97) and there was significant interanimal variation. The mean regenerative index showed that, on average, around 40% of axons grew across the interface and penetrated at least as far centrally as the deep level of the glial dome (Ramer et al. 2002). This compares with regeneration indices close to zero in non-treated material. The possibility remains that axon branching might occur central to the CNS–PNS interface, though it was not seen. This, if it took place, would artificially raise the regeneration index.

In the central tissue compartment of non-treated material, very occasional axons, which by their morphology and position gave the appearance of undergoing regeneration, were seen by systematic searching. It may be that they were central segments of regenerating fibres which had succeeded in penetrating the CNS–PNS interface in the absence of NT3 treatment. If this is so, then the influence of neurotrophin is quantitative rather than qualitative: it enhances (admittedly very markedly so on the basis of the present evidence) the very weak potential for this crucial step in regeneration. In practical terms, however, NT3 is an essential element for functionally effective recovery in this protocol.

These findings show that NT3 is very probably a causal factor in the ingrowth of regenerating axons into the CNS. These studies did not indicate what proportion of the axons reach into the grey matter to set up functional connections, since it was confined to the TZ and its immediate neighbourhood. However, the correlated findings (Ramer et al. 2000, 2002) show that a substantial proportion of these axons do extend deep enough into the CNS to establish functional connections within the dorsal horn grey. There remains, however, a remote possibility that some of the axons have grown in a centrifugal direction, a possibility raised by earlier rigorous studies (Carlstedt et al. 1988, 1989). However, correlated functional, immunohistochemical

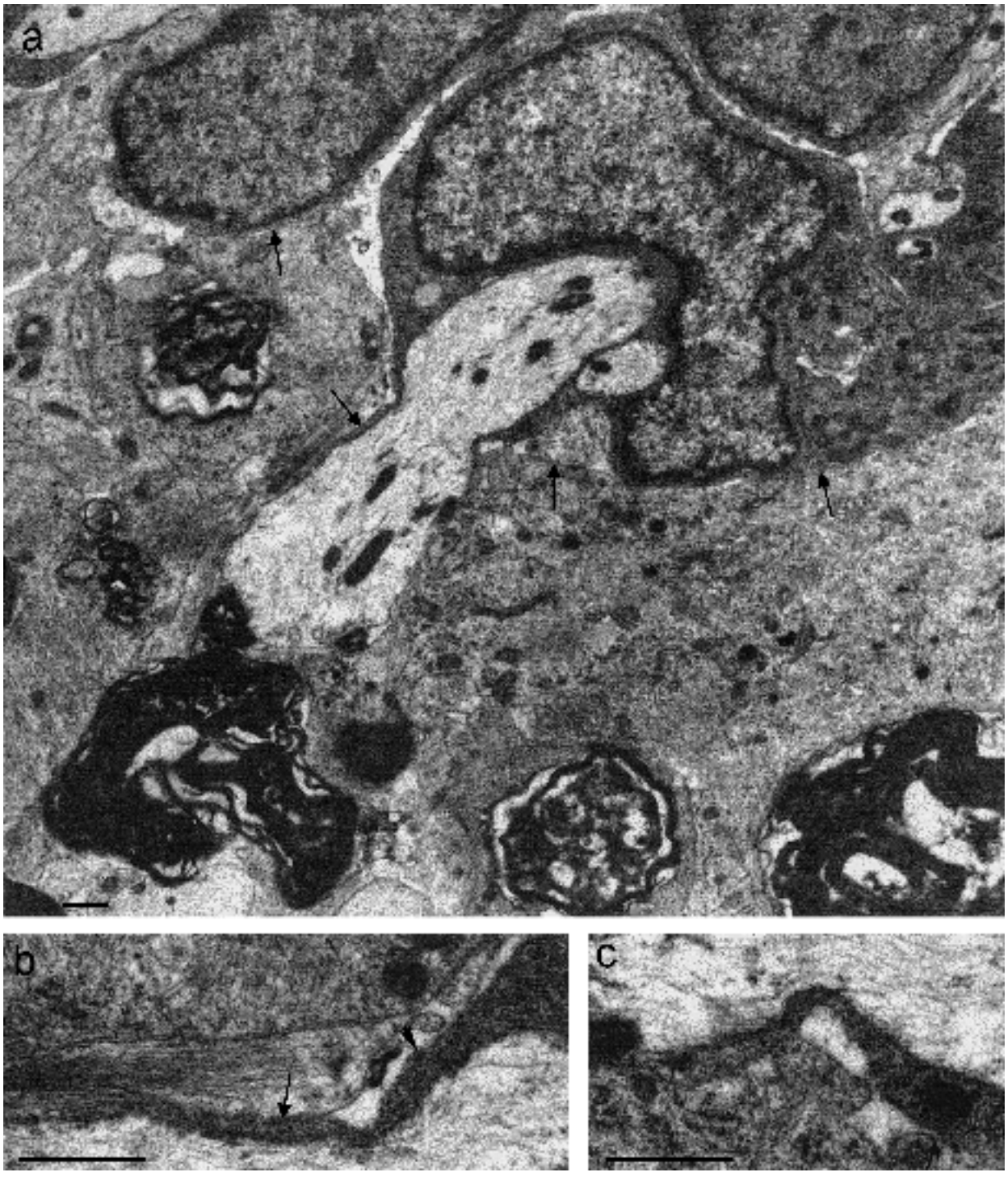


**Fig. 10** (a) An axon traversing the CNS–PNS interface is enveloped peripherally by a rounded Schwann cell perikaryon (above), which is closely related to the glia limitans (arrows) without the intervention of basal lamina. (b,c) Enlargements of (a) showing Schwann cell tongues extending deep to the plane of the CNS surface. These are closely apposed to the astrocyte processes of the glia limitans. Scale bars: 0.5 μm. (a) modified from Ramer *et al*. (2002); (c) from Fraher & Dockery (2002)

and immuno-EM studies from the same series of experiments (Ramer et al. 2002) provide conclusive evidence that a significant proportion of the axons traversing the interface in NT3-treated material do so in a centripetal direction. The regenerative indices inherent in the DRTZ model permit uniquely objective comparison of the relative efficacy of NT3 treatment vs. no treatment. The model will permit comparison of the value of other

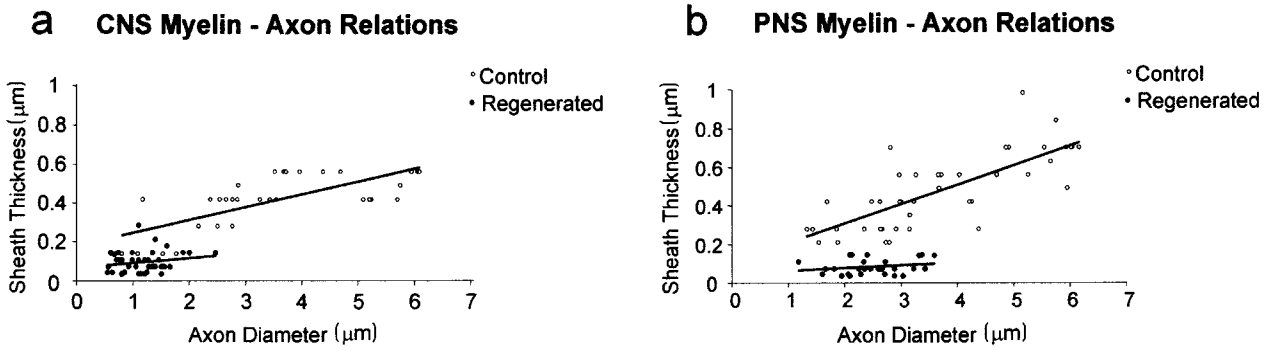


**Fig. 11** Scattergrams showing the relationships between myelin sheath thickness and axon diameter in regenerating (1 week post-operation) and control axons in (a) CNS and (b) PNS. Linear regression lines: CNS normal: $y = 0.07x + 0.18$; regenerating: $y = 0.03x + 0.07$. PNS normal: $y = 0.10x + 0.11$; regenerating: $y = 0.01x + 0.05$. Note the differences between control and experimental groups in the regression line positions and slopes. The slope for the regenerating fibres did not show statistically significant differences from zero. (Modified from Fraher & Dockery, 2002)

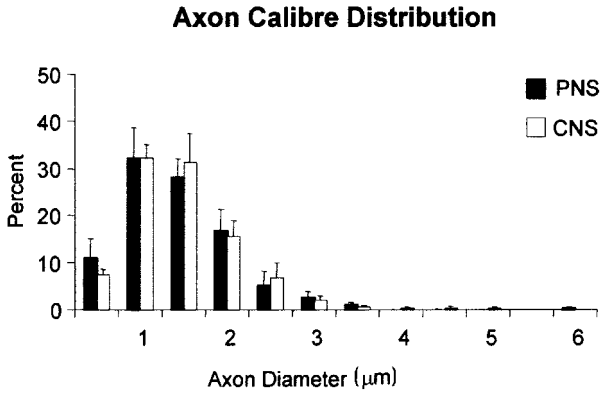


**Fig. 12** Histograms showing diameter distribution of regenerating axons at PNS and CNS levels of NT3-treated specimens. (From Ramer et al. 2002)

competing protocols for achieving the crucial goal of penetrating the CNS surface and growing for some distance through its interstitial space.

As the axons regenerated in a central direction in the PNS, they were enfolded by Schwann cells, or lay within astrocyte – Schwann cell complexes (Fig. 9). In either case, they lay within the tubes of basal lamina which surrounded these complexes and which were continuous at the CNS surface with that on the external surface of the glia limitans (Fig. 9). When they regenerated successfully into the CNS, they did so without piercing the basal lamina. Indeed they may have entered the CNS by traversing the interface in the loci formerly occupied by transitional axons prior to degeneration. Some indications were found that they might even have followed former axonal trajectories in the CNS. This is suggested by the finding that their courses (they tended to run just under the glia limitans surface for a distance after piercing it) resembled that of normal axons within this part of the CTP. It could therefore be that they were following the pathways pursued by axons prior to injury. This cannot be answered on the present evidence, though it is an intriguing possibility.

In another related study in the series, cultured olfactory ensheathing cells (OECs) were injected in suspension into the spinal cord at the point at which a transected adult rat dorsal root was re-sutured to the cord. Animals recovered function in the operated myotomes (Ramon-Cueto et al. 1993; Ramon-Cueto & Nieto-Sampedro, 1994). The TZs of some of the operated roots possessed characteristic complexes of axons and ensheathing cells (Nieto-Sampedro & Taylor, unpublished observations) (Fig. 13). These complexes interdigitated with glial outgrowths related to the TZ and extended centrally for some distance into invaginations of the TZ astrocytic tissue. However, the axons were not followed through the CNS–PNS interface. Half of the complexes consisted exclusively of non-myelinated axons. Around one-tenth consisted of myelinated axons. The remainder were mixed. The myelin sheaths were relatively thin for the associated axon calibre. One-fifth of all complexes contained a blood vessel (Fig. 13a). The ensheathing cells resembled Schwann cells. Their appearance was compatible with that seen in relation to axons undergoing remyelination by OECs in demyelinated spinal cord lesions (Franklin et al. 1996; Franklin & Barnett, 1997, 2000) or in tissue culture (Devon & Doucette, 1992). The axons, and the blood vessels, where present, were surrounded by incomplete sleeves consisting of extended cytoplasmic profiles lacking a basal lamina (Fig. 13b,c).

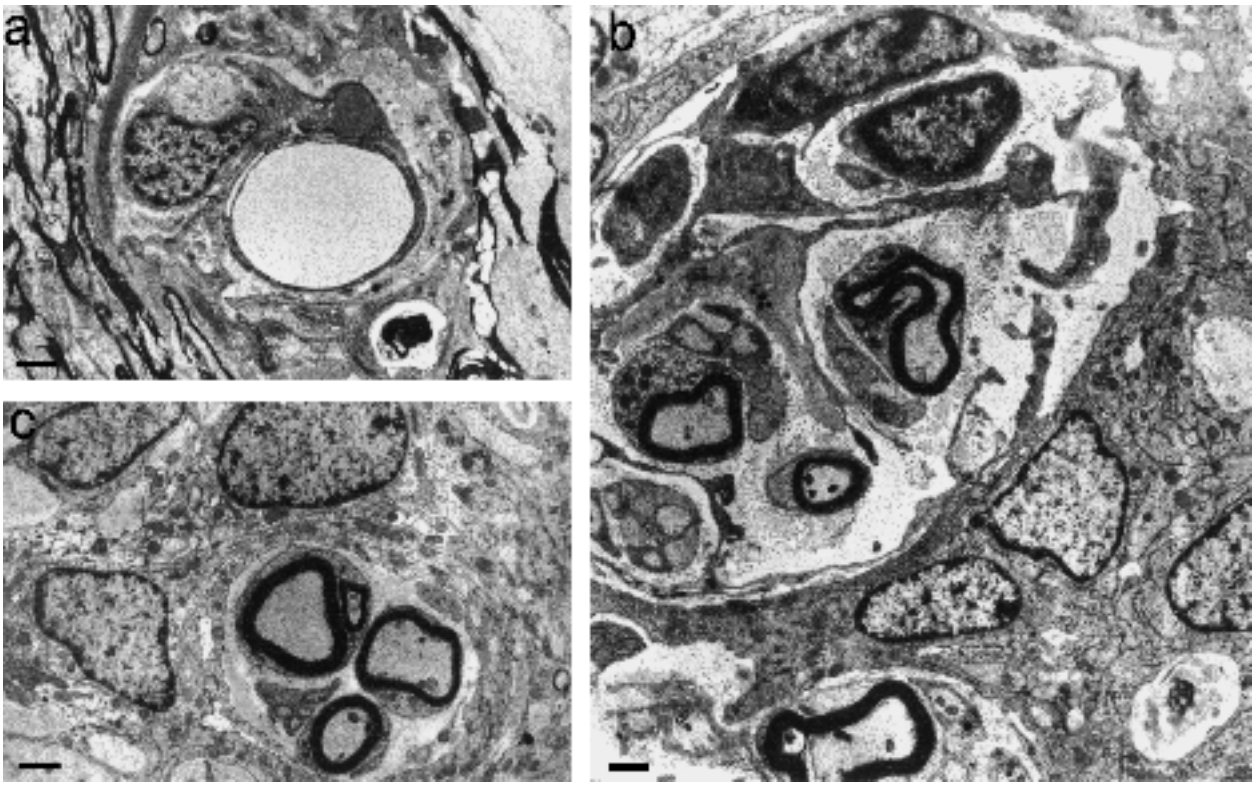


**Fig. 13** Transverse sections of complexes found in regenerating dorsal root TZs, following section and re-suture, combined with OEC injection. (a) These commonly contain blood vessels. (b) Some complexes are large and, in addition to axons, contain a variety of extended cytoplasmic profiles lacking a basal lamina, some of which are arranged circumferentially. (c) Many profiles are smaller, but contain myelinated as well as non-myelinated axons. Myelin sheaths possessed up to 15 lamellae. Scale bars: 1.0 μm.

Some of these projected into the bundle, partly subdividing it. In overall appearance, these features were reminiscent of those found in regenerating rat corticospinal fibre bundles (Li & Raisman, 1993; Li et al. 1997; Raisman, 1997), also associated with injected OECs. It supports the possibility that regeneration across the spinal cord surface is facilitated by the presence of OECs.

## Acknowledgments

I am grateful to the following co-workers: Dr Peter Dockery, Dr Matt Ramer, Dr Makarim Mobarak, Dr Don O'Leary, Dr Siobhan McMahon, Ms Bereniece Riedewald, and to Ms Miriam Dorgan. This work was supported by the EU Biomed programme and by the Wellcome Trust.

## References

**Berthold C-H, Carlstedt T, Corneliuson O** (1984) Anatomy of the nerve root at the central-peripheral transitional region. In: *Peripheral Neuropathy* (eds Dyck PJ, Thomas PK, Lambert EH, Bunge R), Vol. 1, pp. 156–170. Philadelphia: W.B. Saunders.

**Bovolenta P, Wandosell F, Nieto-Sampedro M** (1992) CNS glial scar tissue: a source of molecules which inhibit central neurite outgrowth. In: *Progress in Brain Research* (eds Yu ACH, Hertz L, Norneberg MD, Sykova E, Waxman SG), Vol. 94, pp. 367–379. Netherlands: Elsevier Science.

**Bovolenta P, Wandosell F, Nieto-Sampedro M** (1993) Neurite outgrowth inhibitors associated with glial cells and glial cell lines. *Neuroreport* **5**, 345–348.

**Carlstedt T** (1985a) Regenerating axons form nerve terminals at astrocytes. *Brain Res*. **347**, 188–191.

**Carlstedt T** (1985b) Dorsal root innervation of spinal cord neurons after dorsal root implantation into the spinal cord of adult rats. *Neurosci*. *Lett*. **55**, 343–348.

**Carlstedt T, Dalsgaard C-J, Molander C** (1987) Regrowth of lesioned dorsal root nerve fibers into the spinal cord of neonatal rats. *Neurosci*. *Lett*. **74**, 14–18.

**Carlstedt T** (1988) Reinnervation of the mammalian spinal cord after neonatal dorsal root crush. *J*. *Neurocytol*. **17**, 335–350.

**Carlstedt T, Aldskogius H, Rosario C** (1988) Mammalian root-spinal cord regeneration. *Prog*. *Brain Res*. **78**, 225–229.

**Carlstedt T, Cullheim S, Risling M, Ulfhake B** (1989) Nerve fibre regeneration across the CNS–PNS interface at the root-spinal junction. *Brain Res*. *Bull*. **22**, 93–102.

**Carlstedt T** (1997) Nerve fibre regeneration across the peripheral-central transitional zone. *J*. *Anat*. **190**, 51–56.

**Caroni P, Schwab ME** (1988a) *Two* membrane protein fractions from rat central myelin with inhibitory properties for

neurite growth and fibroblast spreading. *J. Cell Biol*. **106**, 1281–1288.

**Caroni P, Schwab ME** (1988b) Antibody against myelin associated inhibitor of neurite growth neutralises non-permissive substrate properties of CNS white matter. *Neuron* **1**, 85–96.

**Devon R, Doucette R** (1992) Olfactory ensheathing cells myelinate dorsal root ganglion neurites. Brain. *Research* **589**, 175–179.

**Doucette R** (1984) The glial cells in the nerve fiber layer of the rat olfactory bulb. *Anat. Record* **210**, 385–391.

**Doucette R** (1991) PNS-CNS transitional zone of the first cranial nerve. *J. Comparative Neurol*. **312**, 451–466.

**Doucette R** (1993) Glial cells in the nerve fiber layer of the main olfactory bulb of embryonic and adult mammals. *Microsc. Res. Technique* **24**, 113–130.

**Flood PR** (1966) A peculiar mode of muscular innervation in Amphioxus. Light and electron microscopic studies of the so-called ventral roots. *J. Comparative Neurol*. **126**, 181–127.

**Flood PR** (1968) Structure of the segmental trunk muscle in Amphioxus. *Z. Zellforschung* **84**, 389–416.

**Fraher JP** (1973) A quantitative study of anterior root fibres during early myelination. II. Longitudinal variation in sheath thickness and axon circumference. *J. Anat*. **115**, 421–444.

**Fraher JP** (1982) The ultrastructure of sheath cells in developing rat vomeronasal nerve. *J. Anat*. **134**, 149–168.

**Fraher JP, Kaar GF** (1984) The transitional node of Ranvier at the junction of the central and peripheral nervous systems. An ultrastructural study of its development and mature form. *J. Anat*. **139**, 215–238.

**Fraher JP, Kaar GF, Bristol DC, Rossiter JP** (1988) Development of ventral spinal motoneurone fibres. *Prog. Neurobiol*. **31**, 199–239.

**Fraher JP, Rossiter J** (1990) Intermingling of central and peripheral nervous tissues in rat dorsolateral vagal rootlet transitional zones. *J. Neurocytol*. **19**, 385–407.

**Fraher JP** (1992) The CNS-PNS transitional zone in the rat. Morphometric studies at cranial and spinal levels. *Prog. Neurobiol*. **38**, 261–316.

**Fraher J, Cheong E** (1995) Glial – Schwann cell specialisations at the central – peripheral nervous system transition of a Cyclostome: an ultrastructural study. *Acta Anat*. **154**, 300–314.

**Fraher J** (1997) Axon-glial relationships in early CNS–PNS transitional zone development: an ultrastructural study. *J. Neurocytol*. **26**, 41–52.

**Fraher J** (2000) The transitional zone and CNS regeneration. *J. Anat*. **196**, 37–158.

**Fraher JP, Dockery P** (2002) Injury-induced changes in spinal root transitional zones. In: *Glial Interfaces in the Nervous System* (eds Aldskogius H, Fraher J). The Netherlands: IOS Press.

**Franklin RJM, Gilson JM, Franceschini IA, Barnett SC** (1996) Schwann cell-like myelination following transplantation of an olfactory bulb-ensheathing cell line into areas of demyelination in the adult CNS. *Glia* **17**, 217–224.

**Franklin RJM, Barnett SC** (1997) Do olfactory glia have advantages over Schwann cells for CNS repair? *J. Neurosci. Res*. **56**, 665–672.

**Franklin RJM, Barnett SC** (2000) Olfactory ensheathing cells and CNS regeneration; the sweet smell of success? *Neuron* **28**, 15–18.

**Friede RL, Samorajski T** (1968) Myelin formation in the sciatic nerve of the rat. A quantitative electron microscopic, histochemical and radioactive study. *J. Neuropathol. Exp. Neurol*. **27**, 546–571.

**Fritsch B, Northcutt RG** (1993) Cranial and spinal nerve organisation in Amphioxus and lampreys: evidence for an ancestral craniate pattern. *Acta Anat*. **148**, 96–109.

**Guest JD, Hesse D, Schnell L, Schwab ME, Bunge MB, Bunge RP** (1997) Influence of IN-1 antibody and acidic FGF-fibrin glue on the response of injured corticospinal tract axons to human Schwann cell grafts. *J. Neurosci. Res*. **50**, 888–905.

**Kozlova EN, Rosario CM, Stromberg I, Bygdeman M, Aldskogius H** (1995) Peripherally grafted human fetal dorsal root ganglion cells extend axons into the spinal cord of adult host rats by circumventing dorsal root entry zone astrocytes. *Neuroreport* **6**, 269–272.

**Kozlova EN, Seiger A, Aldskogius H** (1997) Human dorsal root ganglion neurons from embryonic donors extend axons into the host rat spinal cord along laminin-rich peripheral surroundings of the dorsal root transitional zone. *J. Neurocytol*. **26**, 811–822.

**Li Y, Raisman G** (1993) Long axon growth from embryonic neurons transplanted into myelinated tracts of the adult rat spinal cord. *Brain Res*. **629**, 115–127.

**Li Y, Field PM, Raisman G** (1997) Repair of adult rat corticospinal tract by transplants of olfactory ensheathing cells. *Science* **277**, 2000–2002.

**Liu L, Kozlova EN** (2000) Glial cell proliferation in the spinal cord after dorsal rhizotomy or sciatic nerve transection in the adult rat. *Exp. Brain Res*. **131**, 64–73.

**O'Brien D, Dockery P, McDermott K, Fraher JP** (1998) The ventral motoneuron axon bundle in the CNS – a cordone system? *J. Neurocytol*. **27**, 247–258.

**O'Brien D, Dockery P, McDermott K, Fraher JP** (2001) Early development of rat ventral root transitional zone: An immunohistochemical and morphometric study. *J. Neurocytol*. **30**, 11–20.

**Pindzola RR, Doller C, Silver J** (1993) Putative inhibitory extracellular matrix molecules at the dorsal root entry zone of the spinal cord during and after root and sciatic nerve lesions. *Exp. Neurol*. **156**, 34–48.

**Raisman G** (1997) Use of Schwann cells to induce repair of adult CNS tracts. *Rev. Neurol*. **153**, 521–525.

**Ramer MS, Priestley JV, McMahon SB** (2000) Functional regeneration of sensory axons into the adult spinal cord. *Nature* **403**, 312–316.

**Ramer MS, Bishop T, Dockery P, Mobarak M, O'Leary D, Fraher JP, et al.** (2002) Neurotrophin-3 promotes functional regeneration of sensory axons into the deafferented adult spinal cord. *Mol. Cell. Neurosci*. in press.

**Ramon-Cueto A, Perez J, Nieto-Sampedro M** (1993) In vitro enfolding of olfactory neurites by p75 NFG receptor positive ensheathing cells from adult rat olfactory bulb. *Eur. J. Neurosci*. **5**, 1172–1180.

**Ramon-Cueto A, Nieto-Sampedro M** (1994) Regeneration into the spinal cord of transected dorsal root axons is promoted by ensheathing glia transplants. *Exp. Neurol*. **127**, 232–244.

**Schnell L, Schwab ME** (1990) Axonal regeneration in the rat spinal cord produced by an antibody against myelin-associated neurite growth inhibitors. *Nature* **343**, 269–272.

**Schwab ME** (1996a) Molecules inhibiting neurite growth: a minireview. *Neurochem. Res*. **21**, 755–761.

**Schwab ME** (1996b) Bridging the gap in spinal cord regeneration. *Nature-Medicine* **2**, 976–977.

**Schwab ME, Brosamle C** (1997) Regeneration of lesioned corticospinal tract fibers in the adult rat spinal cord under experimental conditions. *Spinal-Cord* **35**, 469–473.

**Spillmann AA, Amberger VR, Schwab ME** (1997) High molecular weight protein of human central nervous system myelin inhibits neurite outgrowth: an effect which can be neutralized by the monoclonal antibody IN-1. *Eur. J. Neurosci.* **9**, 549–555.

**Tatagiba M, Brosamle C, Schwab ME** (1997) Regeneration of injured axons in the adult mammalian central nervous system. *Neurosurgery* **40**, 541–547.

**Thallmair M, Metzgas, Z'Graggenw Raineteau O, Kartje GL, Schwab ME** (1998) Neurite growth inhibitors restrict plasticity and functional recovery following corticospinal tract lesions. *Nature Neurosci.* **1**, 124–131.

**Williams PL, Wendell-Smith CP** (1971) Some additional parametric variations between peripheral nerve fibre populations. *J. Anat.* **109**, 505–526.